RESEARCH ARTICLE

Low-carbon strategy of computer numerical control gear hobbing machine based on data-driven combination model and multi-objective optimization strategy

Jiafeng Zhang*

Department of Intelligent Manufacturing Engineering, Meizhouwan Vocational Technology College, Putian, Fujian, China.

Received: June 18, 2024; **accepted:** October 8, 2024.

The computer numerical control gear hobbing machine emits a large amount of carbon dioxide during the actual processing and production, which seriously affects the ecological environment. The study proposed a data-driven combinatorial prediction model and constructed a multi-objective optimization strategy model for the predicting the carbon emission of the gear hobbing machine as well as reducing the production cost. The proposed model combined various prediction models such as support vector machines and artificial bee colony algorithms. The results showed that the average fitness of the optimal solution model computed by Pareto had a maximum value of 90 and a minimum value of 26.31. The value of optimal fitness was constant at 23.56. The maximum value of carbon emission prediction of the proposed model was 1.0 Kg, and the minimum value was 0.37 Kg. The study applied the model to the actual gear hobbing process, and the fitness value converged with only 135 iterations. After 135 iterations, the value remained constant at -14. The cost of machining decreased as the carbon emission increased and the cost was the highest at 0.69 Kg carbon emission, which indicated that the proposed multi-combination drive prediction model was more accurate for carbon emission prediction of computer numerical control gear hobbing machine. Additionally, the approach performed better when it came to improving the multi-objective model, which offered crucial technical support for the machinery manufacturing sector's goal of reducing emissions and saving energy.

Keywords: carbon emissions; forecast; hobbing machine; support vector machine; sparrow search algorithm; adaboost.

***Corresponding author:** Jiafeng Zhang, Department of Intelligent Manufacturing Engineering, Meizhouwan Vocational Technology College, Putian 351100, Fujian, China. Email: zhangjf_1642@163.com.

Introduction

The issue of global warming has become increasingly problematic in recent times. The primary factor contributing to the planet's rising temperature is the increase in carbon dioxide emissions into the atmosphere. The results of a survey indicated that the United States continued to be the world's biggest emitter of carbon dioxide, making up 23.7% of global emissions. About 11.73 tons of carbon dioxide are emitted annually per person in China, which makes up roughly 13.9% of the world's total [1]. The China Ministry of Industry and Information Technology has put forward two key points around the carbon reduction target. One is to promote the development of low-carbon manufacturing and reduce crude steel production. The second is to urge the transformation and upgrading of related

industries [2]. In this context, the machine manufacturing industry has identified a significant challenge of the achievement of low-carbon manufacturing and environmental awareness within the green manufacturing sector while maintaining a balance between economic and environmental benefits [3]. The production and processing of gear instruments consumes a considerable quantity of energy. Some studies examined the potential for reducing energy consumption in computer numerical control gear hobbing machines (CNCGHMs). However, existing manufacturing machines including the CNCGHM have not considered the loss of the machine itself in their studies of low-carbon emission (CE) reduction [4, 5].

The low CE reduction of CNCGHM has attracted the attention of many scholars both domestically and internationally. Hu *et al*. discovered that accuracy was a crucial metric in assessing the effectiveness of machine tools and accuracy distribution in contemporary machine tool design. A MOO algorithm was then suggested to solve the model. The results showed that the algorithm accomplished a thorough optimization of both machining precision and manufacturing cost [6]. Zou *et al*. found that hob wear adversely affected the stability of dry hobbing accuracy and proposed a new strategy for tool wear to collect representative values of power consumption data throughout the development of thermal deformation. The results indicated that the accuracy of this online monitoring method of hob wear condition could reach more than 90% [7]. Liu and Zhu identified that upgrading the working model of non-circular gears became more and more important with the increasing demand for non-circular gears. The results showed that the model was more detailed for gear processing [8]. Ren *et al*. addressed the issue of the inspection process being extremely time-consuming utilizing precision measuring centers by proposing a framework for online evaluation of hobbing quality based on correlation-concerned vibration monitoring to evaluate gear profile deviation and gear lead deviation [9]. Wu *et al*. proposed a helical gear machining parameter optimization method for the problem that the use of unreasonable parameters in dry machining would lead to high cost. The method required the establishment of a three-objective optimization model of efficiency-cost-accuracy. The results indicated that the method had stronger adaptive multi-objective capability and training multi-objective parameters was more advantageous [10].

Predictive models (PMs) are diverse and used in a variety of sophisticated domains. Brunton *et al*. identified an urgent need for safety-critical applications to incorporate machine learning techniques that were interpretable, generalizable, and certifiable. The results revealed that this innovative proposal had made a significant contribution to changing the scientific and industrial landscape [11]. Peng *et al*. found that inaccurate dimensions of composite laminates could affect the overall quantization framework and proposed a data-driven polynomial chaotic unfolding model. The results showed that the model was highly applicable and could be used for multiscale buckling analysis, intrinsic frequency calculation, and reliability assessment [12]. To solve the issue of damage detection in multi-component and composite buildings, Pagani and Enea proposed a convolutional neural network-based building block model that created massive databases through finite element Monte Carlo simulations of randomly damaged structures and found that the model had a significant advantage for damage identification [13]. Kalina *et al.* found that materials with complex underlying microstructures could not be modeled efficiently, so a new data-driven multiscale framework was proposed. The core of the framework was that the entire loop would mine the required dataset completely autonomously. The results indicated that the proposed framework minimized the number of time-consuming microscale simulations [14]. Data-driven approaches garnered a lot of interest in materials research. Wang *et al*. suggested using deep learning and data-driven methods to determine some

performance connections for polymer nanocomposites and found that the model could successfully integrate the driving model while learning, increasing the effectiveness of learning [15].

Gear processing machine tools are highly technical and complex machine tool systems. GHM is one of the most widely used instruments in gear processing machine tools. The traditional mechanical GHM transmission has the disadvantages of low efficiency, poor precision, slow cutting speed, complex operation, and CE seriously over the standard [16]. Previous studies have proposed various optimization strategies for low-carbon operations of gear hobbing machines (GHMs). However, few studies have combined more than three or more PMs. This study suggested a multicombination-driven carbon emission prediction (CEP) model, which consisted of a combination of support vector machine (SVM), support vector regression (SVR), sparrow search algorithm (SSA), and adaptive boosting algorithm (Adaboost). Subsequently, a multi-objective optimization (MOO) function was employed to optimize the strategy of CNCGHM for CEs. Further, the study optimized the prediction of the multi-objective model to achieve accurate prediction of CE for CNCGHM and reduce the cost of energy consumption. This study combined the advantages of the four PMs to predict all aspects of GHM processing with improved accuracy.

Materials and methods

Presets for data-driven combinatorial modeling of CNCGHMs

CNCGHM transmission performance is improved in all aspects to reduce CE and energy consumption. The fully automatic CNCGHM achieved digital control on all six motion axes (a, b, c, x, y, and z axis) necessary for GHM. Its addition of the U-axis and V-axis realized automatic loading and unloading fully automatic control [17]. Processing instruments were accompanied by CE. Due to the long working cycle of the entire gear processing and the complexity of the process, it is hard to predict the CE of the CNCGHM. Therefore, the study started the calculation from its driving model, collected the basic values, and gradually formed the complete CE data set, which was used for the superposition calculation. The study took the complete production process of a gear as a life cycle and focused on each step of its resource consumption. Meanwhile, the study divided such losses into two types of CE, material flow and energy flow, which made it easy to visually distinguish and record the emissions of different processes. The CE operation model of GHM constructed in the study was shown in Figure 1.

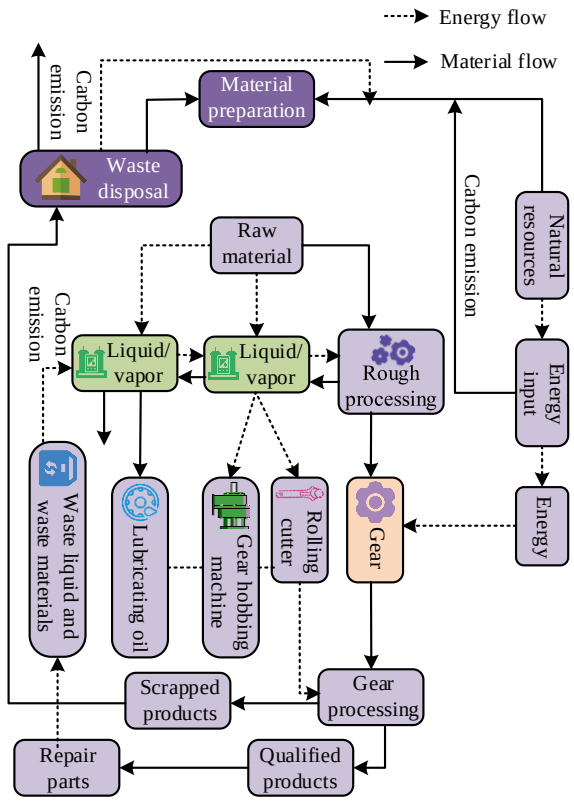

Figure 1. The carbon emission operation model of the gear hobbing machine.

The main energy consumption of CNCGHM can be categorized into machine power system and machine auxiliary system, which contains 12 types of consumption systems such as main

spindle mechanical drive, table mechanical drive, cooling power drive, and so on [18]. Based on this, the study carried out a preliminary design of the CEP model of GHM with multiple linear regression model (MLRM) and logistic regression PM. The MLRM was suitable for calculations with more variables as below.

$$W = \beta_0 + \beta_1 Z_1 + \beta_2 Z_2 + \mathrm{L} + \beta_i Z_i \quad (1)$$

where W was the outcome variable derived from the calculation. Z was the initial variable imported by the calculation. β was the angular coefficient corresponding to the variable indicator. β_0 was the interception range in the operational module. The logistic regression PM was effective in predicting the probability, which was calculated as follows.

$$\frac{dx}{dt} = rx\left(1 - \frac{e}{p}\right) \quad (2)$$

where *t* was the time that the model needed to predict. *x* was the CE generated during operation. *e* was the risk factors during operation. *p* was the maximum acceptable CE generated by the whole prediction session. Combined prediction-driven models could combine the strengths of each PM to achieve more accurate predictions. SVM algorithm is currently mainstreamed in data review, image processing, risk prediction, *etc*. due to its excellent generalization ability significantly [19]. The operation logic of SVM algorithm was to calculate at least one global optimal solution first, and then ensured that all the global training data had the shortest displacement distance from the global optimal solution with the calculation formula below.

$$\omega g + h = 0 \quad (3)$$

where ω was the normal vector. g was the coordinates of the training data. h was the offset degree. Then the position of this data point (DP) to the optimal solution was shown in Equation (4).

$$d = y_a\left(\omega \cdot x_a + b\right) \geq 1 \quad (4)$$

where x_a and y_a were the location of the global optimal solution. d was the shortest distance by which the location of the upper boundary of the optimal solution range was introduced.

$$y_a = +1, \omega \cdot x_a + b \geq +1 \quad (5)$$

In Equation (5), the location of the lower boundary of the optimal solution range was given by Equation (6).

$$y_a = -1, \omega \cdot x_a + b \leq -1 \quad (6)$$

The DPs in the boundary range were collectively referred to as support vectors. The larger the spacing between the support vectors, the better the prediction. The calculation of distance maximization was shown in Equation (7).

$$\begin{cases} \min\limits_{\omega,b} \varphi\left(\omega\right) = \dfrac{1}{2}\|w\|^2 \\ y_a\left(\omega x + b\right) \geq +1 \end{cases} \quad (7)$$

where φ was the distance between the two DPs at the nearest location of the lower and upper boundaries. $\|w\|$ was the separation distance between the upper and lower boundaries. The phenomenon of positional distance discrepancy that occurred in SVM would result in the loss of data that was not within the maximum range of the optimal solution, thereby introducing a bias in the predictions made. SVR modeling algorithm could effectively solve this problem as shown below.

$$f\left(i+1\right) = \sum_{i=1}^{n} (\alpha_i^{\mathrm{g}} - \alpha_i) \cdot Z\left(x_a \cdot x_n\right) + b \quad (8)$$

where α_i was the Lagrange multiplier. $f\left(i+1\right)$ was the decision classification model. Z was the model computational power. After the driving model combined SVM and SVR algorithm models, it still lacked the warning system and the

adaptive effect was poor. Therefore, the research again proposed to incorporate the sparrow algorithm into the driving model. The fundamental concept of SSA was to partition the search space into many subspaces, and then search each subspace independently until the target was located or the search space was emptied [20]. The SSA calculation was shown in Equation (9).

$$X_{i,j}(t+1)=\begin{cases} X_{i,j}(t)\cdot\exp\left(-\dfrac{i}{\alpha\cdot t_{\max}}\right), if \quad J<SE \\ X_{i,j}(t)+Q\cdot R \qquad\qquad , if \quad J\geq SE \end{cases} \tag{9}$$

where $X_{i,j}$ was the DP location. J was the alert value of the prediction range. SE was the safe value of the prediction range. R was the element matrix. Q was the random number when the data were normally distributed. After the early warning system was integrated into the prediction-driven model, the model function tended to be perfect in the theoretical sense. However, the model had to take into account the false indications produced by the weak learner during training, and corrections needed to be made in time. Adaboost classification could effectively solve the weak learner information classification problem and could be calculated as follows.

$$Z_m=\sum_{i=1}^{N} w_{mi}\exp\left(-\alpha_m y_a G_m(x_a)\right) \tag{10}$$

where Z_m was the specification factor. α_m was the weight coefficient. $G_m(x_a)$ was the weak classifier. w_{mi} was the enhanced classification factor. Then, the upper error limit of the Adaboost could be deduced and calculated as below.

$$E_m=\max\left|y_a-G_m(x_a)\right|, a=1,2,\mathrm{L}\ ,N \tag{11}$$

where E_m was the computation-time error ratio of the weak classifier. The addition of Adaboost brought a qualitative improvement to the overall drive PM performance. Therefore, the SSA-AVM-Adaboost model was transported in four steps including finding the best solution, a weak learner of the Adaboost model; training to extract the number of weak learners; computing and training the parameters as well as the learners by combining the first two steps; outputting the training results and putting them in use. The operational flow of the CDPM proposed in the study was shown in Figure 2.

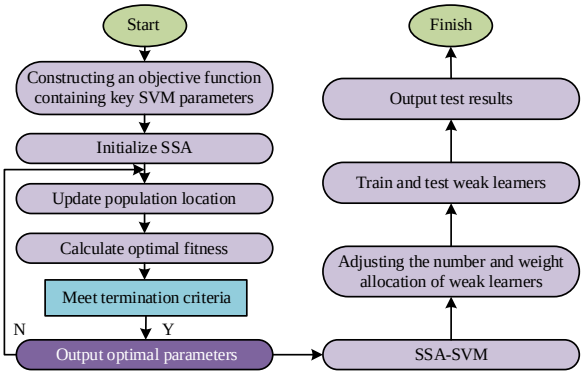

Figure 2. The operational flowchart of the combination driven prediction model.

Multi-objective low-carbon optimization strategy for CNCGHMs

After the initial construction of the CDPM, the CE of the GHM was also able to be initially predicted. In the process of machining and making gears in CNCGHM, there were many sources of CE, and the definition was complicated, often involving the machine tool itself emissions including heat production, idling, on and off, *etc*., as well as the lubrication system involved in machining raw materials. The data resources in this study were based on the YS3120CNC6 model hobbing machine equipment and workpiece technical table (Chongqing Machine Tool Group Co., Ltd., Chongqing, China). The parameter information in the data table was used as the initial value applied to the actual experiment. The entire machine process of a machine tool involved a large number of emission objectives. Therefore, multi-objective CE nodes needed to be optimized. The key to judging the effectiveness of

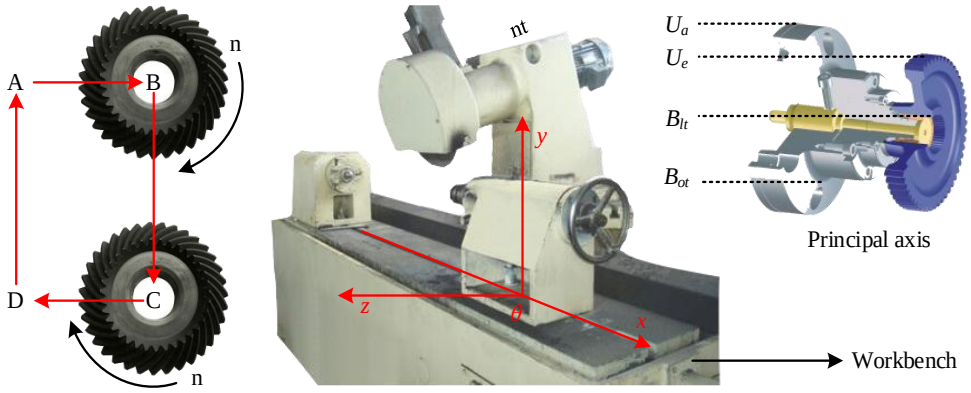

Figure 3. Cutting status of gear hobbing machine after adding constraint conditions.

CNCGHM's CE control was to evaluate tool wear, which was also a complex aspect of CE. The machining tool loss was proportional to the length of the machining time, and its cost was calculated as follows.

$$Z_1 = \sum_{i \in n} \frac{t_{oi}}{T_{ti}} W_{Ti} h_t \tag{12}$$

where Z_1 was tool cost. h_t was tool price. T_{ti} was the tool life. W_{Ti} was the actual quality of the tool. t_{oi} was the tool replacement frequency. The CE function for hobbing was shown in Equation (13).

$$Q_2 = \sum_{i \in n} B_i \tag{13}$$

where Q_2 was the total amount of CE for the production of the n th roller. B_i was the individual CE of the n th gear. Cutting volume was the main consumption of CE. Controlling the range of cutting amount and constraining the numerous variables could control the total CE more effectively. The cutting force constraint was calculated below.

$$T_c \le T_{\max} \tag{14}$$

where T_c was the cutting force constraint. The equipment power constraint of CNCGHM was calculated as shown in Equation (15).

$$R_b \le \sigma R_{\max} \tag{15}$$

where R_b was the power constraint of CNCGHM. σ was the sum of the motor power of the spindle and the power supplied to the motor. The model's forecast of the CE was significantly more accurate when the multi-objective PM fell inside the restrictions. The cutting process after adding constraints was shown in Figure 3. The spindle hob speed n of the GHM was expanded in the y-axis. The worktable was used as a platform for instrument carrying and workpiece machining. The workpieces needed to be conveyed into the GHM from the z-axis. The trajectory of the hob operated cyclically around the four points of A, B, C, and D. The hob needed to pass through the hob front distance B_{lT}, the cut-out safety distance U_e, the existing travel distance $B_{oT,}$ and the cut-out safety distance U_a. After the cutting process was optimized, there were still multi-objectives to be optimized. The Pareto optimal solution (POS) space was chosen to further handle the MOO problem (Figure 4). The study assumes two objective functions. For solution ×4, no other solution could be found in the variable space that could outperform solution ×4, and solution ×4 was the POS. Moreover, no solution could be found in the entire solution space that was closest to the origin. Then solution ×1 was also the optimal solution. The study took advantage of the optimization of POS for multi-objective problems and adapted the PM. Eventually, the CNCGHM machining process model was built for

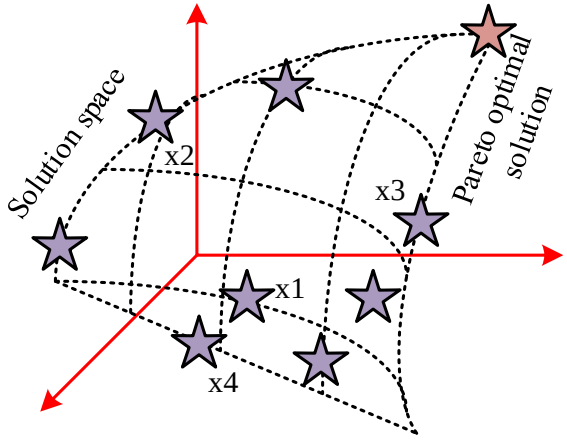

Figure 4. Pareto optimal solution operation space. The purple pentagram was the listed solutions. The red pentagram represents the POS. The net circled range indicated the objective space.

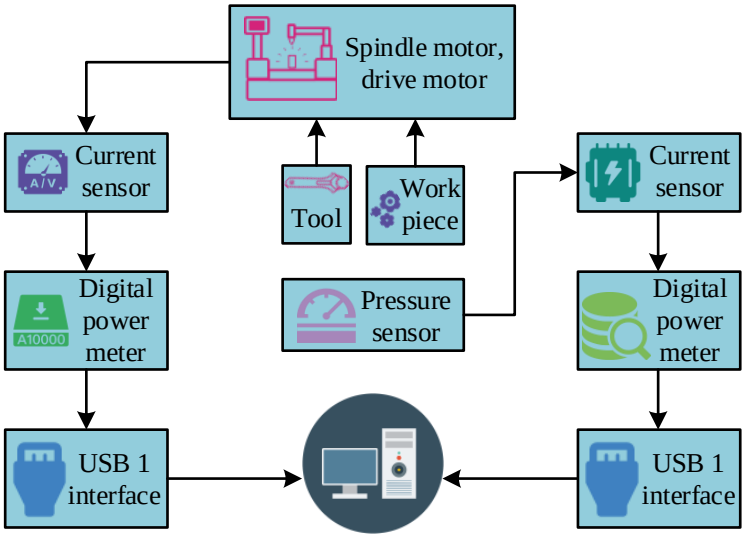

Figure 5. Optimization of multi-objective system for CNC gear hobbing machine.

minimizing the cost of machining gear loss and CE, and multi-constraint multi-objective based on the theory (Figure 5).

To verify whether the combined PM of SSA-SVR-SVM-Adaboost proposed by the study was more accurate in predicting the CE of CNCGHM, a series of comparison experiments were performed using Intel® Xeon® Platinum 8124M, 64 GB RAM, Windows 10, 64-bit operating system, C++, and Matalab2018b (MathWorks, Natick, Massachusetts, USA). 100 sets of data were randomly sampled to ensure that the parameters of the processed gear samples were consistent. The training sample set consisted of 50 sets and the test sample set consisted of the remaining 50 sets. In addition, to verify the degree of carbon emission optimization of the model in multi-objective production, four commonly used cloud manufacturing algorithms including artificial bee colony algorithm (ABC), improving the bee colony algorithm (IABC) for model research, particle swarm optimization (PSO), and ant colony optimization (ACO) were selected for path optimization, financial prediction, and multi-objective comparison.

Table 1. Variable parameter settings for SSA-SVR-SVM-Adaboost combination prediction model.

Variable parameters	Numerical value	Variable parameters	Numerical value
Population size N_P	20	Maximum number of iterations *T*	100
Penalty parameters C	[0.01, 100]	Safety value *ST*	0.6
Discoverer ratio *PD*	0.7	Proportion of guards *SD*	0.2
Cross validation fold *V*	5	Width parameter *g*	[0.01, 1,000]

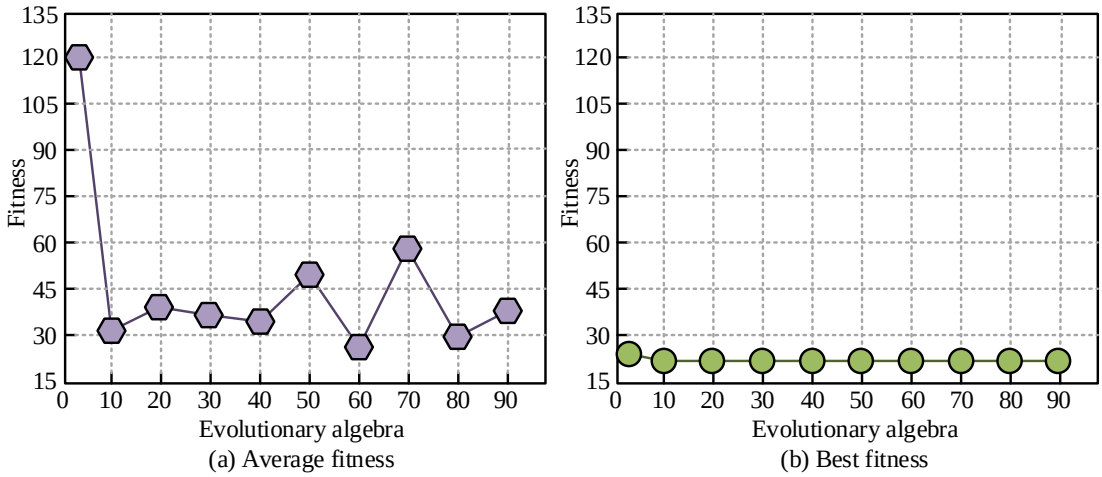

Figure 6. Optimal solution fitness value curve.

Results and discussion

Performance analysis of CNCGHM based on data-driven combination model and multi-objective optimization strategy

The algorithmic configuration and the restriction parameters used in the study for the proposed model were shown in table 1. 50 sets of test data were imported into the combined PM of SSA-SVR-SVM-Adaboost model. The model was executed in a sequence that began with the determination of the range of solutions and subsequently progressed to the identification of the optimal solution. The root mean square error in the value of the fitness function was employed as the evaluation index. The average fitness (AF) value of the final optimal solution range and the best fitness value were shown in Figure 6. The AF curve of the model varied greatly with the AF value showing an extremely fast decreasing trend until the number of iterations reaching 5 and a minimum and maximum values of 26.31 and 90, respectively (Figure 6a). The optimal fitness curve of the model showed an overall smooth trend, which only floated and changed before 3 iterations reaching a maximum value of 25. After 3 iterations, the value of the optimal fitness was constant at 23.56 (Figure 6b), which resulted in a penalty parameter of 15.55 and a width parameter of 1.9 for the optimal fitness. The optimal fitness of the proposed model was less variable and had a high degree of adaptation. In addition, three different PMs including SSA-SVR-SVM-Adaboost, SVM, and artificial neural network (ANN) were selected to further validate the prediction performance of the proposed model. The results showed that the lowest CE for the proposed model was studied in the training set with a maximum value of 1.7 Kg and a minimum value of 0.38 Kg (Figure 7a). The overall CE curve for SSA-SVR-SVM-Adaboost had less variation compared to the other two PMs and was the closest to the true CEP value curve. The maximum predicted value of CE for the SVM algorithm model appeared between 0 and 5 sample points as 2.3 Kg, and the minimum value

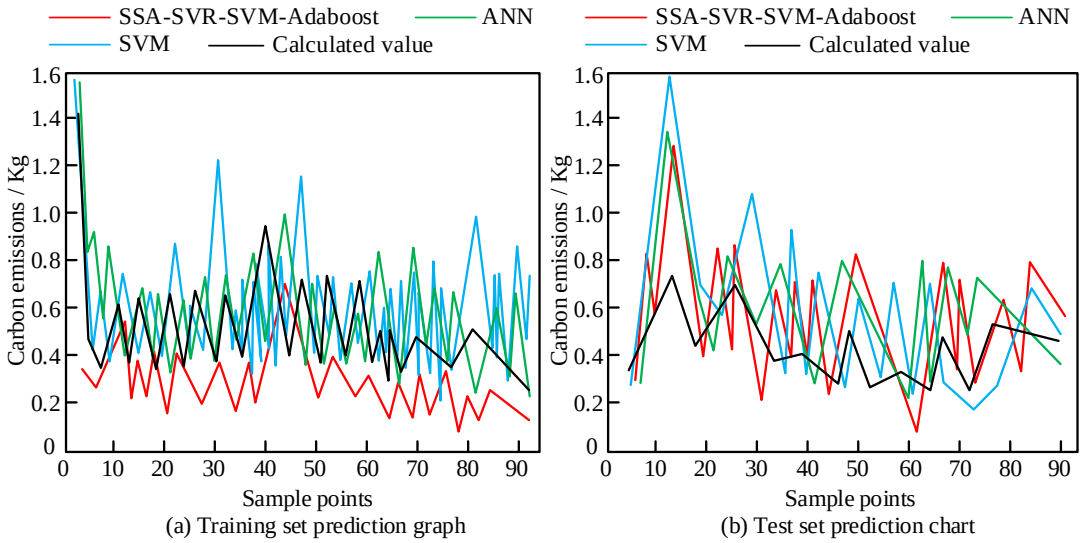

Figure 7. Comparison of carbon emissions between the training and testing sets.

appeared between 15 and 20 sample points as 0.56 Kg. The fluctuation of the ANN model curve was done large, and the minimum and the maximum values were 2.5 Kg and 0.44 Kg, respectively, which were consistent with the SVM appearing intervals. The CEP curve of the proposed model was the closest to the real predicted curves in distance. The maximum value of CEP of the proposed model appeared between 0 and 5 sample points as 1.0 Kg, and the minimum value appeared between the 10th sample points as 0.37 Kg (Figure 7b), which suggested that the proposed model's accuracy matched the real value.

The optimization of CNCGHM for practical applications

The proposed model was further evaluated by the actual GHM machining process for its practical application. The logarithmic change in fitness values for two single-peak tests of four algorithms applied to a 50-dimensional operating environment was shown in Figure 8. Two test functions, f1 and f2, were selected to compare the logarithmic change in the single-peak fitness value. As the iterations increased, IABC required the least iterations to reach the convergence effect, and the adaptation value converged with only 135 iterations with a constant value of -14 (Figure 8a). The PSO and ACO algorithms demonstrated similar effects and had not converged for the time being. The ABC curve showed a trend of regular convergence. The number of iterations used for the convergence of IABC for f2 was less compared to f1, and the curve stabilized after only 21 iterations with the value being constant at -15 after 45 iterations (Figure 8b). The other three algorithms, except ACO, only ABC and PSO algorithms showed a tendency to converge after 400 iterations, and the results were unsatisfactory. The results indicated that the algorithms of proposed model had better convergence at single-peak values when applied in practice. The convergence of the four algorithms of f1 was close to the single peak curve. The iterations used for the convergence of IABC remained the least with 45 iterations, and the value of the subsequent iterations stabilized around -16. PSO did not show any convergence for the time being. ACO converged slowly, and the effect was not obvious. ABC convergence effect was better than PSO and ACO, but the same convergence trend was not obvious. IABC had a better effect of convergence trend (Figure 9a). IABC converged with the least number of iterations, which started to converge rapidly at 9 iterations with a value of -16.5. The convergence trend of ABC showed a stepwise decline and

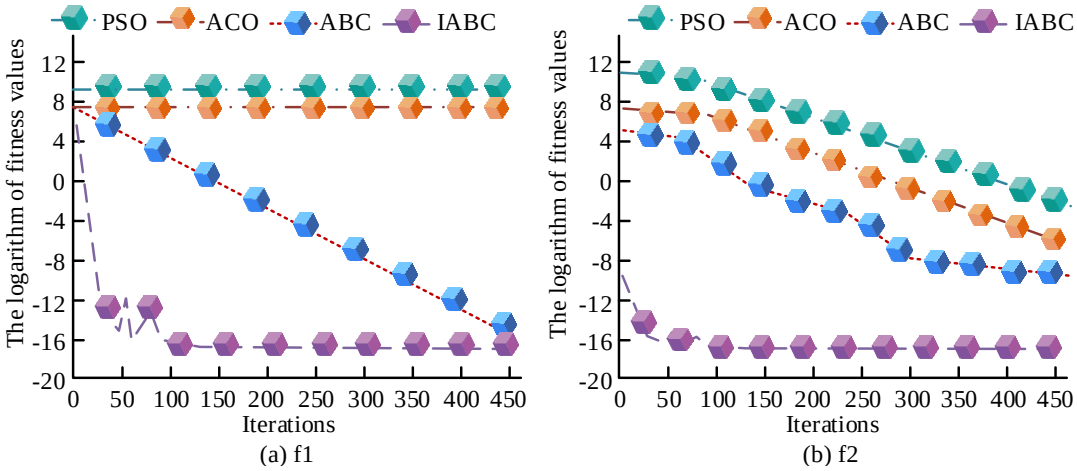

Figure 8. Convergence curve of unimodal test function.

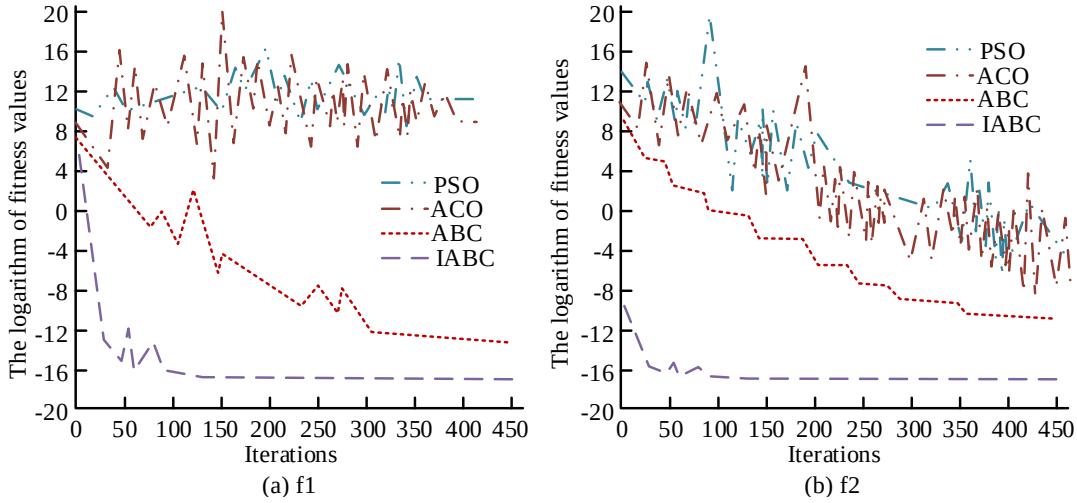

Figure 9. Convergence curve of multimodal test function.

eventually stabilized at 460 iterations with a value of -13. The PSO and ACO algorithms both did not have any trend of convergence, and the convergence effects were poor (Figure 9b). To further verify the superiority of the proposed model for MOO, the study introduced a fast non-dominated sorting genetic algorithm 2 (NSGA2) to simulate and analyze the comparison with IABC. The Pareto frontier solution range of IABC was larger than the optimal solution of NSGA2, which suggested that IABC could dominate all the optimal solutions of the domain class. The optimization of cutting parameters by IABC decreased the machining cost as the CE increased, and the cost was the highest at 0.69 Kg CE (Figure 10a). The NSGA2 Pareto frontier optimal solution range curve was second to IABC. The results showed that the proposed model had great advantages both in terms of its ability to predict CE and multi-objective parameter optimization, which was effective in reducing CE as well as saving cost of CNCGHM (Figure 10b).

The SSA-SVR-SVM-Adaboost multi combination drive CNCGHM CEP model proposed in the study utilized IABC and NSGA2 to calculate the POS of the multi-objective optimization model. Among the 100 sets of randomly sampled data, the AF

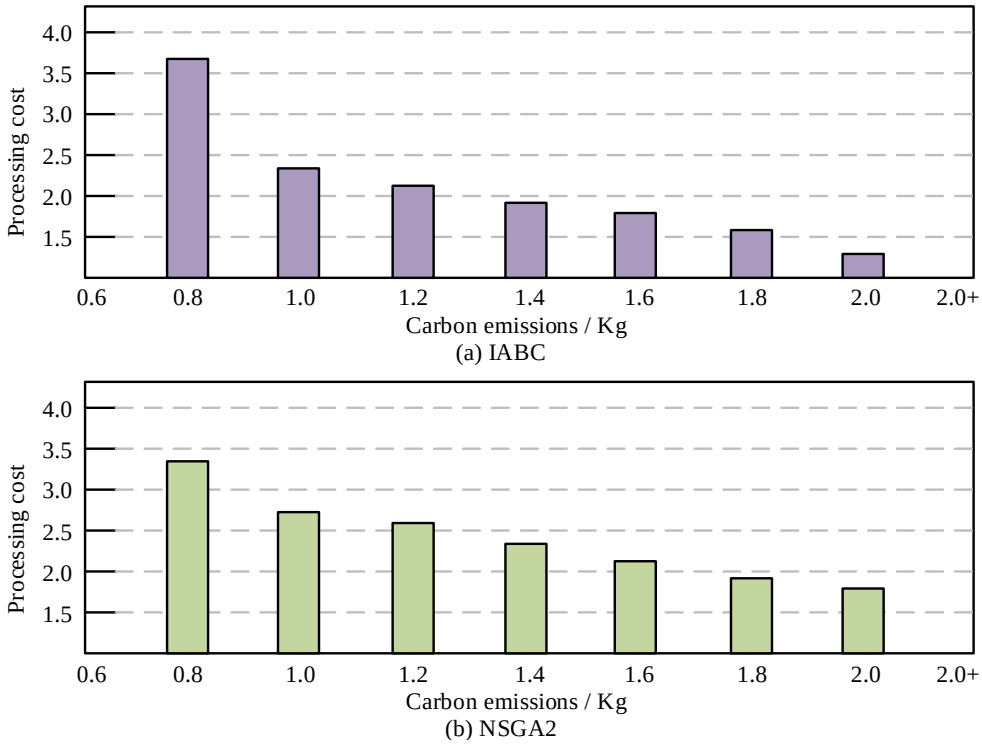

Figure 10. Pareto frontier carbon emissions and corresponding cost comparison.

value of the optimal solution model showed a rapid downward trend before 5 iterations. The maximum value was 90 at 0 iterations, and the minimum value was 26.31 between 60 and 80 iterations. Zhang *et al*. also obtained similar results through experimental calculations, indicating that the fitness range difference of the optimal solution of the proposed model was relatively small [21]. The maximum fitness value of the model before 3 iterations was 25. Moreover, after 3 iterations, the optimal fitness value remained constant at 23.56. The penalty parameter for optimal fitness was 15.55, while the width parameter was 1.9. A constant fitness required fewer iterations, indicating strong adaptability of the model. The carbon emissions of the model proposed in the training set were the lowest with a maximum value of 1.7 Kg occurring between 20 and 25, and a minimum value of 0.38 Kg occurring between 25 - 30. Liang *et al*. compared the carbon emissions of GHMs by proposing a model and finally obtained approximate results [22], which indicated that the combination drive prediction model proposed by the research was more suitable for CEP scenarios of CNCGHMs with the most accurate prediction results. It could minimize processing costs and optimize the multi-objective model to the greatest extent possible.

References

1. Wu Z, Zhao Y, Zhang N. 2023. A literature survey of green and low-carbon economics using natural experiment approaches in top field journal. GLCE. 1(1):2-14.
2. Amer M, Wojcik EZ, Sun C, Hoeven R, Hughes JM, Faulkner M. 2020. Low carbon strategies for sustainable bio-alkane gas production and renewable energy. Energ Environ Sci. 13(6):1818-1831.
3. Hu Z, Wang S, Ma C. 2023. Precision allocation method of large-scale CNC hobbing machine based on precision-cost comprehensive optimization. Int J Adv Manuf. 126(7):3453-3474.
4. Zhang Y, Liu Y, Wang Y, Liu D, Wang Z, Liu Y. 2020. Urban expansion simulation towards low-carbon development: A case study of Wuhan. Sustain Cities Soc. 63:102455.
5. Yang B, Liu Z. 2020. Thermal error modeling by integrating GWO and ANFIS algorithms for the gear hobbing machine. Int J Adv Manuf Tech. 109(9):2441-2456.

6. Yi Q, Liu C, Li C, Zhao X, Xu M, Hu C. 2023. A prior knowledge-integrated method of carbon emissions modeling and optimization for gear hobbing with small sample problem. Int J Adv Manuf. 125(3):1661-1678.
7. Zou Z, Cao R, Chen W, Lei S, Gao X, Yang Y. 2021. Development of a tool wear online monitoring system for dry gear hobbing machine based on new experimental approach and DAE-BPNN-integrated mathematic structure. Int J Adv Manuf Tech. 116(1):685-698
8. Liu Y, Zhu LL. 2022. Research on non-circular helical gear NC hobbing linkage control scheme based on variable transmission ratio. P I Mech Eng B-J Eng. 236(11):1433-1442.
9. Ren H, Yin A, Song W, Yang Y. 2020. Vibration monitoring with dependencies attention for gear hobbing quality evaluation. IEEE Sens J. 20(22):13726-13733.
10. Wu D, Yan P, Guo Y, Zhou H, Yi R. 2021. Integrated optimization method for helical gear hobbing parameters considering machining efficiency, cost and precision. Int J Adv Manuf Tech. 113(3):735-756.
11. Brunton SL, Nathan Kutz J, Manohar K, Aravkin AY, Morgansen K, Klemisch J, *et al*. 2021. Data-driven aerospace engineering: reframing the industry with machine learning. AIAA J. 59(8):2820-2847.
12. Peng X, Ye T, Li J, Wu H, Jiang S, Chen G. 2021. Multi-scale uncertainty quantification of composite laminated plate considering random and interval variables with data driven PCE method. Mech Adv Mater Struc. 28(23):2429-2439.
13. Pagani A, Enea M. 2024. Displacement and strain data-driven damage detection in multi-component and heterogeneous composite structures. Mech Adv Mater Struc. 31(9):2053-2068.
14. Kalina KA, Linden L, Brummund J, Kästner M. 2023. FE ANN: an efficient data-driven multiscale approach based on physics-constrained neural networks and automated data mining. Comput Mech. 71(5):827-851.
15. Wang Y, Zhang M, Lin A, Iyer A, Prasad AS, Li X, *et al*. 2020. Mining structure–property relationships in polymer nanocomposites using data driven finite element analysis and multi-task convolutional neural networks. Mol Syst Des En. 5(5):962-975.
16. Singh V, Patra S, Murugan NA, Toncu DC, Tiwari A. 2022. Recent trends in computational tools and data-driven modeling for advanced materials. Materials Advances. 3(10):4069-4087.
17. Boral P, Gołębski R, Kralikova R. 2023. Technological aspects of manufacturing and control of gears. Materials. 16(23):7453.
18. Prasanth A, Jayachitra S. 2020. A novel multi-objective optimization strategy for enhancing quality of service in IoT-enabled WSN applications. Peer Netw Appl. 13(6):1905-1920.
19. Tian Y, Si L, Zhang X, Cheng R, He C, Tan KC. 2021. Evolutionary large-scale multi-objective optimization: A survey. CSUR. 54(8):1-34.
20. Ren Y, Yu J, Zhao A, Ran T, Yang X. 2021. A multi-objective operation strategy optimization for ice storage systems based on decentralized control structure. Build Serv Eng. 42(1):62-81.
21. Zhang C, Li B, Yu C, Li H, Zhu Y. 2024. Prediction of the modal parameters of the spindle system in high-speed dry hobbing machine with thermal effects. AJST. 9(3):221-226.
22. Liang D, Zhao W, Chen Y, Meng S. 2023. Mathematical model and deviation analysis of machining cutters for internal gears with double contact points. P I Mech Eng C-J Mech. 237(13):3103-3114.